American Journal of Optics and Photonics
2016; 4(4): 32-39
http://www.sciencepublishinggroup.com/j/ajop
doi: 10.11648/j.ajop.20160404.12
ISSN: 2330-8486 (Print); ISSN: 2330-8494 (Online)

Configuration Dependent Electronic and Optical Properties of WZ-$CuInS_2$

Bo Gao, Fu-Ling Tang*, Hong-Tao Xue, Fu-Zhen Zhang, Yu-Wen Cheng

Department of Materials Science and Engineering, Lanzhou University of Technology, State Key Laboratory of Advanced Processing and Recycling of Non-ferrous Metals, Lanzhou, China

Email address:

lutgaobo@163.com (Bo Gao), tfl03@mails.tsinghua.edu.cn (Fu-Ling Tang), 309877689@qq.com (Hong-Tao Xue), 1264395734@qq.com (Fu-Zhen Zhang), 1109551346@qq.com (Yu-Wen Cheng)

*Corresponding author

To cite this article:

Bo Gao, Fu-Ling Tang, Hong-Tao Xue, Fu-Zhen Zhang, Yu-Wen Cheng. Configuration Dependent Electronic and Optical Properties of WZ-$CuInS_2$. *American Journal of Optics and Photonics.* Vol. 4, No. 4, 2016, pp. 32-39. doi: 10.11648/j.ajop.20160404.12

Received: September 15, 2016; **Accepted**: October 13, 2016; **Published**: November 3, 2016

Abstract: We used the first-principles calculations based on density functional theory to calculate the electronic and optical properties of wurtzite $CuInS_2$ (WZ-$CuInS_2$) in which the copper and indium atoms share the same lattice site. It is found that WZ-$CuInS_2$ is metallic for local aggregative indium and copper atomic configurations, or is a semiconductor for local even-distributed configurations. Metallic configurations have higher lattice energies while semi conductive configurations have lower lattice energies. As the degree of the local aggregation of Cu and In atoms increases, the band gap of the WZ-$CuInS_2$ decreases. The optical properties of WZ-$CuInS_2$ were also calculated and found that the optical band gap also decreases as local aggregation of Cu and In atoms with increases. The metallic configurations have a higher absorption coefficient.

Keywords: First Principles Calculation, Atomistic Configuration, Electronic Properties, Optical Properties, WZ-$CuInS_2$

1. Introduction

As new members of the photovoltaic materials, I-II-VI_2 semiconductor compounds (for example, $CuGaSe_2$ and $CuInSe_2$) have been well realized [1-3]. For $CuInS_2$ polymorphic structures, chalcopyrite phase (CP-$CuInS_2$) is the most common structure, zincblende phase (ZB-$CuInS_2$) is metastable, and wurtzite phase (WZ-$CuInS_2$) structure was synthesized recently [4, 5]. Unlike in traditional CP-$CuInS_2$ solar cell material, Cu and In atoms randomly share the same lattice site with the same half possibility in WZ-$CuInS_2$ unit cell. This characteristic makes it flexible in stoichiometry and suitable for high-efficient solar cells [6]. Acting as a new valuable solar cell material, WZ-$CuInS_2$ has attracted widespread attentions. Because of its excellent band gap (1.45-1.5 eV) matching with the solar spectrum, it displays higher light absorption efficiency over some other materials [7]. Optimized WZ-$CuInS_2$ solar cells had the conversion efficiency up to 5% at elevated temperatures [8]. In addition, it also has other features, for example, good electrical stability, environment friendly and economic prospects [9-11]. Drawing by these advantages, many research groups recently have devoted to synthesize this material with various nanocrystalline approaches [12-13].

The random distribution of Cu-In in WZ-$CuInS_2$ introduces the flexibility of stoichiometry and possibly makes its Fermi energy easily changed over a wider range [13-15]. Hence, different Cu-In configuration possibly leads to various electronic and optical properties. At present, few theoretical investigations on the electronic and optical properties of WZ-$CuInS_2$ have been carried out, especially, at atomistic level. From common first principles calculation within density functional theory, the lattice and electronic structures can be well obtained, but it couldn't precisely predict band gap and optical properties. The hybrid Hartree-Fock-like functional by Heyd, Scuseria, and Ernzerhof (HSE) can improve the calculation accuracy [16, 17]. Many groups have proven that the HSE06 function made a good description not only for the electronic properties but also for the optical properties [18-23]. So the HSE06 function was used to study the configuration dependent lattice stability and the configuration effect on the electronic and optical properties of WZ-$CuInS_2$.

2. Methodology

The unit cell of CuS (with the space group P63mc, a = 3.906 Å, c = 6.429 Å) was used as the starting point for In-doping calculation. Half of Cu atoms were substituted by In atoms. We prepared many different Cu-In configurations by using the Monte Carlo Alloy Theoretic Automated Toolkit (ATAT) [24-26]. In this work, based on the first principles density functional theory, the Vienna Ab-initio simulation package (VASP) [27-29] was utilized, supplementing with the projector augmented wave (PAW) method [30, 31]. For the pseudopotential that was used, the electronic configurations are [Ar] 3d104s1, [Kr] 5s25p1, and [Ne] 3s23p4 for copper, indium, and sulfur respectively. The plane wave energy cutoff is 410 eV and the Brillouin zone is sampled by an 8×8×5 Monkhorst–Pack k-mesh to calculate these structures. We used the tetrahedron method to calculate the total lattice energy and the density of states (DOS) for all atomistic configurations [32]. In order to obtain their equilibrium structures, the Density Functional Theory (DFT) was used to relax the cell lattice parameters and their ion positions to obtain their lowest energy structures. The HSE06 hybrid functional with Hartree–Fock screening parameter $\omega = 0.2$ was employed to calculate the electronic and optical properties.

The response of matters to electromagnetic fields is described by the complex dielectric function. The dielectric matrix can be calculated on condition that the electronic ground state is determined. The complex dielectric function is a bridge between the microscopic and macroscopic measurements of the material and plays an important role in the study of the optical properties of semiconductors. Using the complex dielectric functions $\varepsilon(\omega)=\varepsilon_1(\omega)+\varepsilon_2(\omega)$ and the absorption coefficient $\alpha(\omega)$, the optical properties can be presented. Then the imaginary part of the dielectric function was calculated using the equation:

$$\varepsilon_{\alpha\beta}^{(2)}(\omega)=\frac{4\pi^2e^2}{\Omega}\lim_{q\to 0}\frac{1}{q^2}\sum_{c,v,k}2w_k\delta(\varepsilon_{ck}-\varepsilon_{vk}-\omega)\times\langle u_{ck}+e_{\alpha q}\left|u_{vk}\right\rangle\langle u_{ck}+e_{\beta q}\left|u_{vk}\right\rangle^* \quad (1)$$

where the indices c is conduction band state, v is the valence band state. Ω is the volume, w_k is the k-point weight, ε_{jk} is the energy state, u_{jk} is the cell periodic part and e_α is the unit vector. Then the real part of dielectric function tensor $\varepsilon_{\alpha\beta}^{(1)}$ was got using KramersKronig transformation:

$$\varepsilon_{\alpha\beta}^{(1)}(\omega)=1+\frac{2}{\pi}P\int_0^\infty\frac{\varepsilon_{\alpha\beta}^{(2)}(\omega')\omega'}{\omega'^2-\omega^2+i\eta}d\omega' \quad (2)$$

where P denotes the principal value and η is an infinitesimal number [33].

3. Results and discussion

In WZ-$CuInS_2$ lattice, the sub-lattice structure is a tetrahedron: S atom at the center and four Cu/In atoms around it. In every tetrahedron, Cu and In atoms may have different occupancies. There must be five and only five possible occupancies in the tetrahedrons, named a, b, c, d, e respectively in Fig. 1. In the tetrahedron a, the S atom is surrounded by two Cu atoms and two In atoms. In b/c, the S atom is surrounded by three/one Cu atom(s) and one/three In atom(s). In d/e, the S atom is surrounded by four Cu/In atoms. All of the WZ-$CuInS_2$ lattices are constituted by some of these five type tetrahedral structures. In addition, the typical bond lengths of In/Cu-S are also shown in Fig. 1.

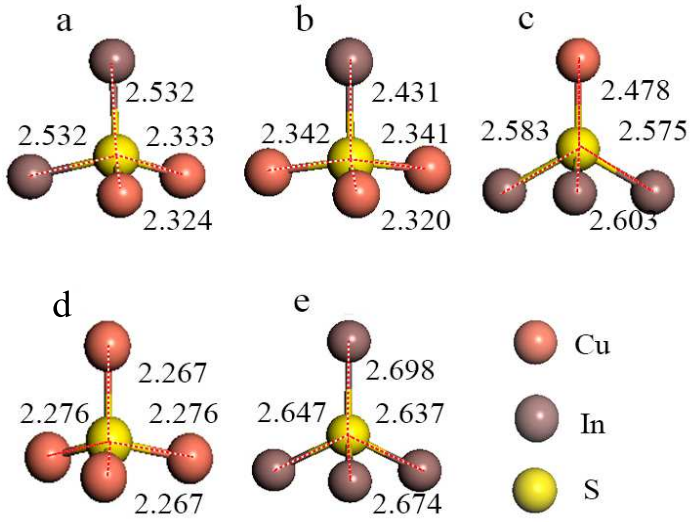

Fig. 1. *Five possible tetrahedral structures in WZ-$CuInS_2$ and their typical bond lengths (Å).*

There are eight WZ-$CuInS_2$ structural configurations with different sub-lattices and their total energies were listed in Table 1. We name five WZ-$CuInS_2$ structures as type I (a-e), and name other three WZ-$CuInS_2$ structures as type II (f-h). Their percentages for tetrahedrons a-e are listed in Table 1. Type I lattices haven't d or e tetrahedron, while Type II lattices have d or/and e tetrahedron. For example, in the lattice structure e of type I, half tetrahedrons are of type b, and the others are of type c. These structures are shown in Fig. 2.

Table 1. *Sub-lattices and total energies of several WZ-$CuInS_2$ structures.*

Lattice structure		a*	b	c	d	e	E_{tot}(eV)
	a	1**	0	0	0	0	-66.56
	b	3/4	1/8	1/8	0	0	-66.35
Type I	c	2/5	3/10	3/10	0	0	-65.98
	d	1/3	1/2	1/6	0	0	-65.84
	e	0	1/2	1/2	0	0	-65.10
	f	1/2	0	1/3	1/6	0	-65.29
Type II	g	1/6	1/6	1/2	1/6	0	-64.92
	h	1/3	1/6	1/6	1/6	1/6	-64.58

*a-e denote the five possible tetrahedral structures in Fig. 1.
**0 to 1 denotes the percentage of every tetrahedral structure (a-e in Fig. 1) in the lattice structure.

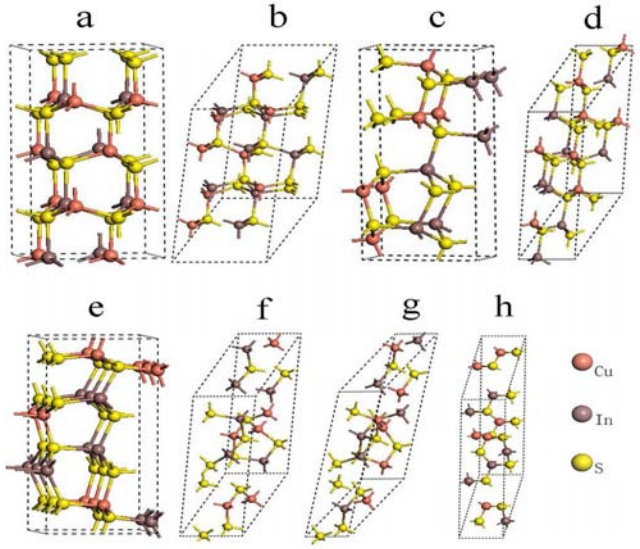

Fig. 2. *WZ-$CuInS_2$ structures in Table 1.*

3.1. Type I WZ-$CuInS_2$

Type I WZ-$CuInS_2$ structures just have a, b, c type tetrahedrons (Fig. 1). For example, structure a (Fig. 2a) just composes the type a tetrahedrons, and has the lowest lattice energy. In fact, this structure is the most stable structure we studied. The atomic stack way of the structure a which is the simplest is: along [0 0 1] direction, the Cu cation and In cation are alternately stacked; along [1 0 0] every S atom bonds to two Cu and two In cations. For the WZ-$CuInS_2$ structure e (Fig. 2e), along [1 0 0] direction, the first layer just contains Cu cations, the second layer contains both Cu cations and In cations; the third layer just contains In cations; and the forth layer again contains both Cu cations and In cations. In such a pattern, the atoms are arranged consecutively and periodically. This means that along [0 1 0] the first S atom is bonded to three Cu and one In cations, and the following S atom is bonded to one Cu and three In cations. While structure e has higher lattice energy, it hasn't the type a tetrahedron. It can be seen that the lattice energy gradually increases as the percentage of type a tetrahedrons reduces.

3.1.1 Electronic Properties

From the density of states (DOS) and band structure diagram, we can judge a system is a metal, semiconductor or insulator from its band gaps. The DOS of structures a-e of type I was got by HSE06, as presented in Fig. 3, and found that the electronic density near the Fermi level increases as the occupancy of type a tetrahedron decreases. From partial density of states (PDOS), we can find that the electronic state near the Fermi level of structure e is formed by 5*s*-orbital of In atoms.

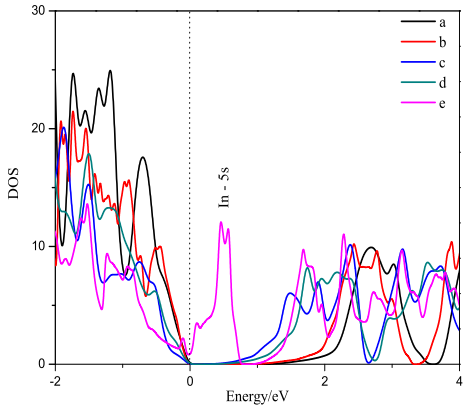

Fig. 3. *Density of states (DOS) of type I, structures a to e.*

The band structure of these configurations, is shown as in Fig.4. The calculated band gap of structure a is about 1.21 eV, which is closer to the experimental band gaps (1.47 eV) [6]. Structure d's band gap is about 0.12 eV and structure e has no band gap at gamma-point. The Fig. 4 shows that structure a-d have direct band gap, in which the top of the valence band and the bottom of the conduction band lie along the gamma-point. As shown in DOS and band structure diagram, the band gap of structures a-d becomes smaller with the decrease of type a

tetrahedron's percentage. Structures a-d exhibit semiconductor properties while structure e has a similar DOS of metals.

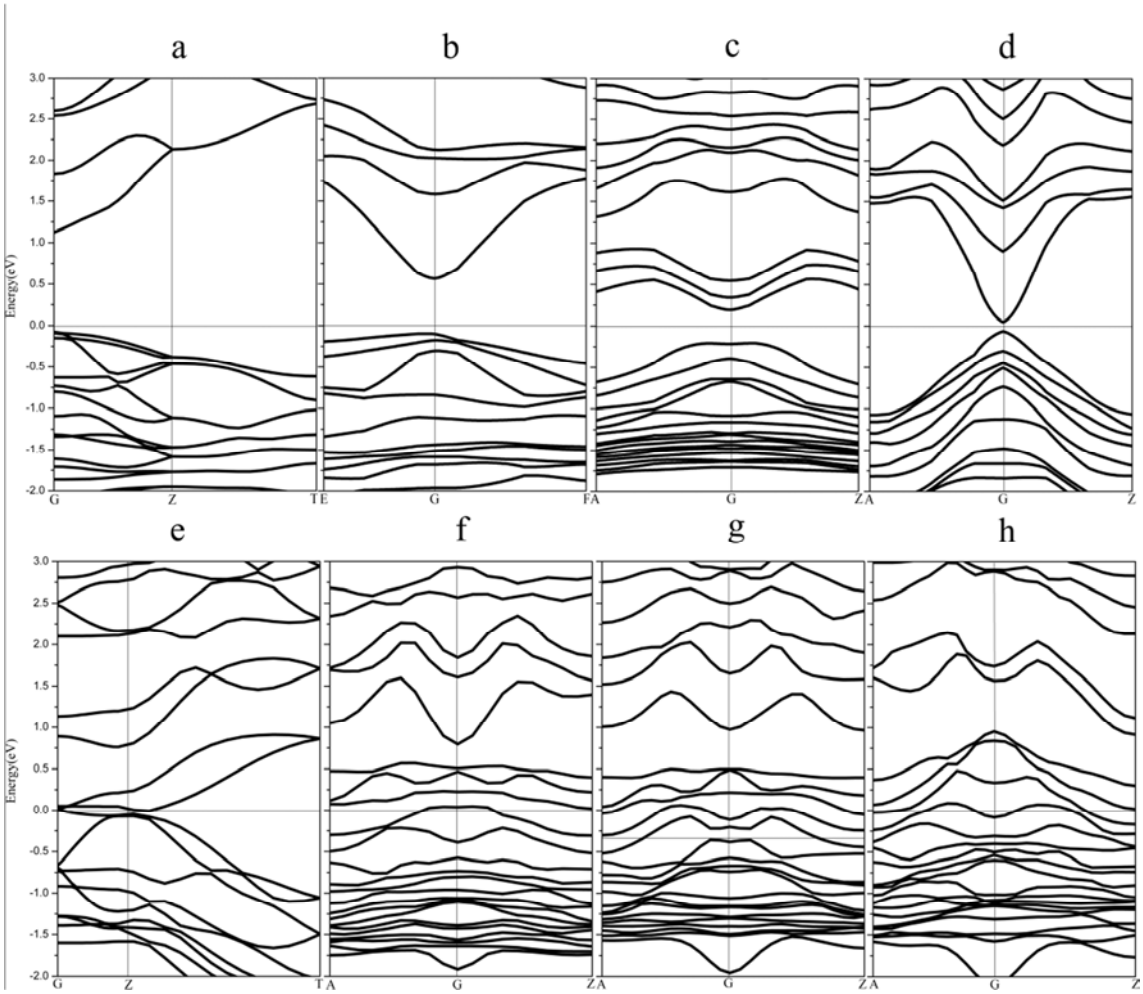

Fig. 4. *Band structure of these structures in Table 1.*

In structure a or e, there are four Cu, four In and eight S atoms. Their Bader's atomic charges are shown in Table 2. For structure a, S atoms gain 0.93 and 0.94 *e* (electrons). Cu and In atoms lose 0.52 and 1.35 *e*, respectively. However, for structure e, S atoms gain 0.88 and 1.10 *e*, and Cu and In atoms lose 0.49 and 1.25 *e*. Compared with structure a, two Cu atoms in structure e lose much more electrons. This may be a reason for their DOS difference in Fig. 3.

Table 2. *Bader's atomic charges in structures a and e.*

Structure	Cu		In		S			
a	0.52	0.52	1.35	1.35	-0.93	-0.93	-0.93	-0.93
	0.52	0.52	1.35	1.35	-0.94	-0.94	-0.94	-0.94
e	0.49	0.50	1.26	1.00	-0.95	-0.99	-1.10	-1.10
	1.35	0.96	1.03	1.25	-0.99	-0.95	-0.88	-0.88

3.1.2. Optical Properties

The absorption coefficient $\alpha(\omega)$ denotes when a beam of light with a particular wavelength illuminates into a material the distance that it can propagate before it is absorbed. Through the dielectric function, the absorption coefficient can be got by this formula:

$$\alpha(\omega)=\sqrt{2}\omega\left[\sqrt{\varepsilon_1(\omega)^2+\varepsilon_2(\omega)^2}-\varepsilon_1(\omega)\right]^{1/2}=2\omega\kappa. \quad (3)$$

The absorption spectra of these structures are given in Fig. 5. The absorption coefficient rises to peak and then slip down. When the photon frequency is larger than 25 eV, it will be close to zero. Structures a-e have similar absorption curves whose peaks appear at 12 eV with a value of $2.5\times10^5 cm^{-1}$. Structure e shows a very special absorption spectra, reaching maximum at about 6 eV with a much higher absorption peak ($4.8\times10^5 cm^{-1}$). Its absorption coefficient is about two times of other structures. From the absorption spectra, the optical band gap can be figured out through the formula: $d[\ln(\alpha h\nu)]/d[h\nu]-h\nu$ ($h\nu$ is the energy of photon [34]). The inset of Fig. 5 displays the relationship between $d[\ln(\alpha h\nu)]/d[h\nu]$ and $h\nu$ for structure a and b. The dotted lines present the values of the optical band gap. Because the optical band gap of other structures is very narrow, we do not show them here. The optical band gap of structure a is about 1.19 eV which is in good accordance with the experimental

result (1.282 eV) [13]. The optical band gap of the structure b is about 1.06 eV. However the structure e hasn't optical band gap, displaying metallic properties. Generally, with the increase of the percentage of type a tetrahedron, the optical band gap decreases, the coefficient of absorption rises. Finally, the structure e exhibits metallic properties.

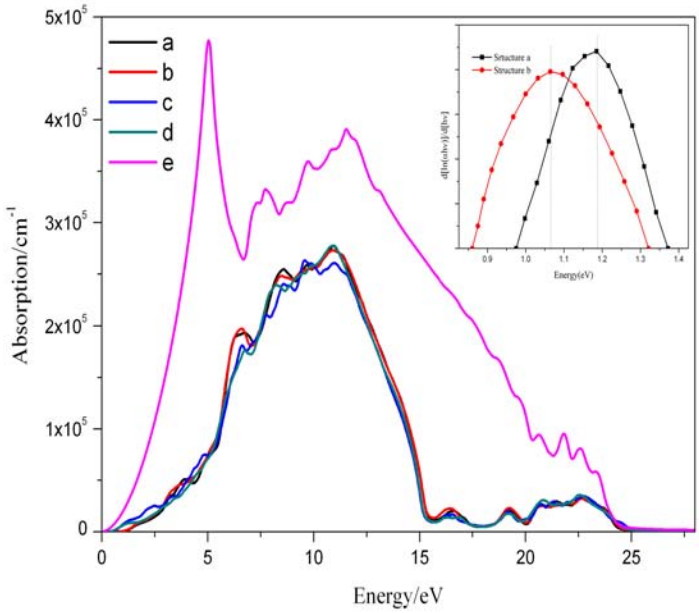

Fig. 5. *Absorption coefficient of the type I structures (a-e) in the ordinary polarization.*

According to the relationship between the complex refractive $N = \sqrt{\varepsilon(\omega)} = n + ik$, the refractive indices n and the extinction coefficient κ, we can get the following two formulas:

$$n = \left(\frac{\sqrt{\varepsilon_1^2 + \varepsilon_2^2} + \varepsilon_1}{2}\right)^{1/2}, \tag{4}$$

$$\kappa = \left(\frac{\sqrt{\varepsilon_1^2 + \varepsilon_2^2} - \varepsilon_1}{2}\right)^{1/2}. \tag{5}$$

The refractive indices of structures a-e are shown in Fig. 6a. With the increase of the energy of the photon, *n* experiences a little decline at first then slightly rises soon later. When the photon energy is large enough, *n* will increase to approximately 0.8. The extinction coefficient of materials can also be found (in Fig. 6b). It rises to peak at which point the photon energy is about 6 eV, and then slip down. Not only the refractive indices but also the extinction coefficient of structure e is quite different from those of structures a-d.

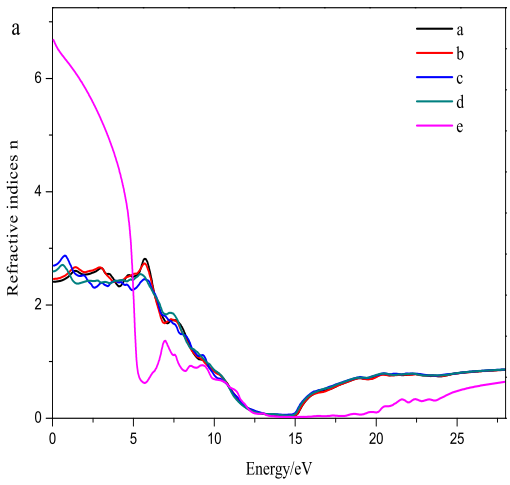

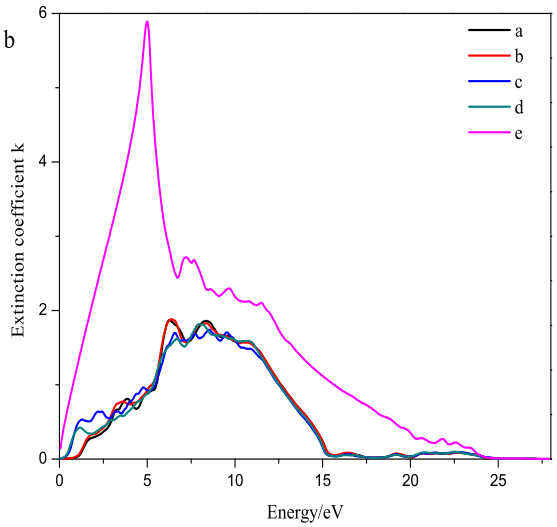

Fig. 6. *Refractive indices (a) and extinction coefficient (b) in the ordinary polarization of structures a-e.*

3.2. Type II WZ-CuInS2

There are three different structures presented in type II, f-h (Table 1). Unlike in type I structures, tetrahedron(s) d and/or e appear in type II structures. In tetrahedron d or e, four Cu or In atoms are aggregative around S atom. In $CuIn_{1-x}Ga_xSe_2$ system, In and Ga atoms are aggregated to form phase separation at low temperature [35]. In $CuIn(Se_{1-x}S_x)_2$ system, Se and S atoms tempt to form phase separation [36].

The structure h is shown in Fig. 2h. This is a more complex structure than others, which contains all the five tetrahedrons. Along [0 0 1], it can be divided into two layers: the first layer contains Cu and S atoms and the second layer contains In and S atoms, and these two layers appear alternatively. Generally, the structures' lattice energies of type II is higher than those of type I structures. In other words, when the indium and copper atoms' distribution is more aggregative, its lattice energy will become higher.

The DOS of type II structures f-h (Fig. 7a) shows that there are density states appearing above the Fermi level. And the electronic state near Fermi level is also from the 5*s*-orbital of In atoms. We can also notice that there is no band gap for structures f-h from Fig. 4. That is to say, they are all metallic. But structure h is more metallic than structures f and g because it has higher density states near the Fermi level. The absorption spectrum is also calculated (Fig. 7b). With the ascending of the energy of the photon, absorption spectrum increases at first but sharply reduces later and tends to be flat eventually. Structures f-h of type II have similar but smaller absorption coefficient compared with those of structures a-d of type I.

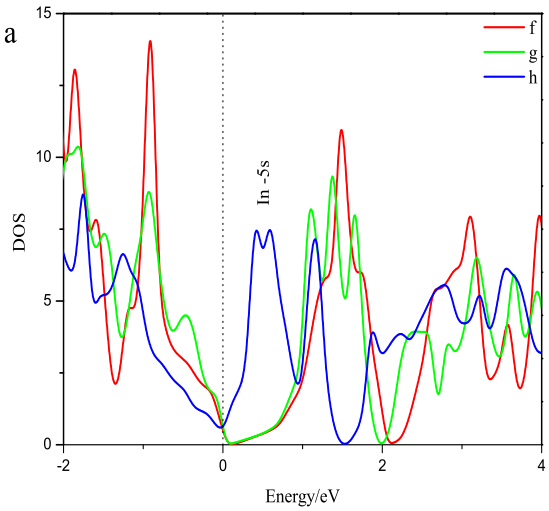

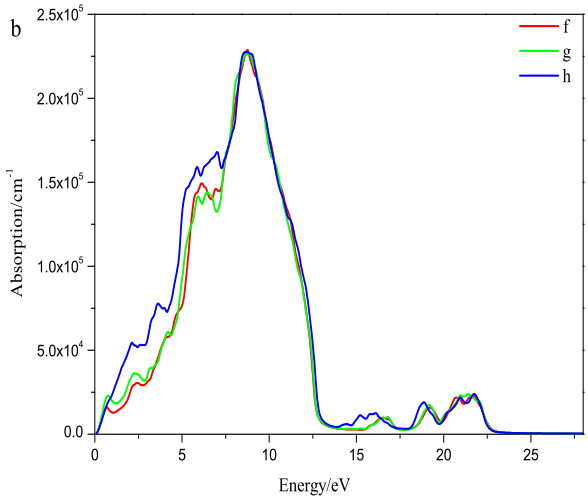

Fig. 7. *DOS (a) and absorption coefficient(b) of type II structures f-h.*

Here we must remind that WZ-$CuInS_2$ attracted many interests recently as a potential semiconductor solar cell material. According to their lattice energies, the experimentally synthesized WZ-$CuInS_2$ may be a mixture of different atomistic configurations. WZ-$CuInS_2$ with local aggregative indium and copper atomic configurations are energically less stable, and its metallic properties may do harm to solar cell performance. Anyway, our studies will be helpful to understand this material. Further experimental and theoretical research is needed to confirm the existence of metallic configurations in WZ-$CuInS_2$ based solar cells, to investigate their effects, and to avoid them.

4. Conclusion

Based on the first-principles calculations we calculated the electronic and optical properties of wurtzite $CuInS_2$ with different local atomic configurations. The main findings are: 1) Cu-In configuration has a significant effect on the stabilities and properties of wurtzite $CuInS_2$. 2) As the degree of the local aggregation of Cu and In atoms increases, the band gap of the WZ-$CuInS_2$ decreases. 3) WZ-$CuInS_2$ is metallic for local aggregative Cu and In configurations, or is a semiconductor for local even-distributed configurations. 4) The lattice energy increases as the system changes from semiconductive to metallic.

Acknowledgement

This work was financially supported by the National Nature Science Foundation of China (11164014 and 11364025). This work was performed in the Gansu Supercomputer Center.

References

[1] Y. Tani, K. Sato and H. Katayama-Yoshida, “First-principles materials design of $CuInSe_2$-based high-efficiency photovoltaic solar cells,” Physica B. vol. 407, pp. 3056-3058, August 2012.

[2] A. A. I. Al-Bassam, “Electrodeposition of $CuInSe_2$ thin films and their characteristics,” Physica B. vol. 266, pp. 192-197, May 1999.

[3] M. I. Alonso, K. Wakita, J. Pascual, M. Garriga and N. Yamamoto, “Optical functions and electronic structure of CuInSe2, CuGaSe2, CuInS2, and CuGaS2,” Phys. Rev. B. vol. 63, pp. 075203, July 2000.

[4] Z. Yin, Z. L. Hu, H. H. Ye, F. Teng, C. H. Yang and A. W. Tang, “One-pot controllable synthesis of wurtzite $CuInS_2$ nanoplates,” Appl. Surf. Sci. vol. 307, pp. 489-494, July 2014.

[5] M. Gusain, P. Kumar and R. Nagarajan, “Wurtzite $CuInS_2$: solution based one pot direct synthesis and its doping studies with non-magnetic Ga^{3+} and magnetic Fe^{3+} ions,” RSC. Adv. vol. 3, pp. 18836-18871, April 2013.

[6] F. F. Zhou, Q. M. Chen, J. Chen, T. T. Wang, Z. Jia, X. M. Dou and S. L. Zhuang, A method for synthesizing wurtzite $CuInS_2$, Optical. Instruments. vol. 36, pp. 342-345, 2014.

[7] M. E. Norako, M. A. Franzman and R. L. Brutchey, “Growth kinetics of monodisperse Cu− In− S nanocrystals using a dialkyl disulfide sulfur source,” Chem. Mater. vol. 21, pp. 4299-4304, August 2009.

[8] D. Cahen, G. Dagan, Y. Mirovsky, G. Hodes, W. Giriat and M. Lubke, “Ternary Chalcogenide - Based Photoelectrochemical Cells IV. Further Characterization of the Polysulfide Systems,” J. Electrochem.Soc. vol. 132, pp. 1062-1070, May 1985.

[9] K.T. Kuo, S.Y. Chen, B.M. Cheng and C. C. Lin, “Synthesis and characterization of highly luminescent $CuInS_2$ and $CuInS_2$/ZnS (core/shell) nanocrystals,” Thin Solid Films. vol. 517, pp. 1257-1261, December 2008.

[10] Z. D. Wang, X. L. Mo, J. Li, D. L. Sun and G. R. Chen, “Low-temperature synthesis and characterization of the single chalcopyrite phase $CuInS_2$ compound by vacuum sintering method,” J. Alloys Compd. vol. 487, pp. 1-2, May 2009.

[11] F. Heidemann, L. Gutay, A. Meeder and G. H. Bauer, "Ensemble analyses by Minkowski-operations for spatially resolved structural and optoelectronic features of Cu (In, Ga)(Se_2, S_2) absorbers," Thin Solid Films vol. 517, pp. 2427-2430, February 2009.

[12] B. Koo, R. N. Patel and B. A. Korgel, "Wurtzite−Chalcopyrite Polytypism in $CuInS_2$ Nanodisks," Chem. Mater. vol. 21, pp. 1962-1966, April 2009.

[13] Y. X. Qi, Q. C. Liu, K. B. Tang, Z. H. Liang, Z. B. Ren and X. M. Liu, "Synthesis and characterization of nanostructured wurtzite $CuInS_2$: a new cation disordered polymorph of $CuInS_2$," J. Phys. Chem. C. vol. 113, pp. 3939-3944, February 2009.

[14] M. Kruszynska, H. Borchert, J. Parisi and J. Kolny-Olesiak, "Synthesis and shape control of $CuInS_2$ nanoparticles," J. Am. Chem. Soc. vol. 132, pp. 15976-15986, October 2010.

[15] D. Pan, L. An, Z. Sun, W. Hou, Y. Yang, Z. Yang and Y. Lu, "Synthesis of Cu− In− S ternary nanocrystals with tunable structure and composition," J. Am. Chem. Soc. vol. 130, pp. 5620-5621, April 2008.

[16] J. Heyd, G. E. Scuseria and M. Ernzerhof, "Hybrid functionals based on a screened Coulomb potential," J. Chem. Phys. vol. 118, pp. 8207, November 2002.

[17] J. Heyd, G. E. Scuseria and M. Ernzerhof, "Erratum: "Hybrid functionals based on a screened Coulomb potential" [J. Chem. Phys.118, 8207 (2003)]," J. Chem. Phys. vol. 124, pp. 219906, April 2006.

[18] J. Paier, R. Asahi, A. Nagoya and G. Kresse, "Cu_2ZnSnS_4 as a potential photovoltaic material: a hybrid Hartree-Fock density functional theory study," Phys. Rev. B. vol. 79, pp. 115126, March 2009.

[19] H. Zhao and C. Persson, "Optical properties of Cu(In,Ga)Se_2 and Cu_2 $ZnSn(S,Se)_4$," Thin Solid Films. vol. 519, pp. 7508-7512, August 2011.

[20] P Deak, B. Aradi and T. Frauenheim, "Polaronic effects in TiO_2 calculated by the HSE06 hybrid functional: Dopant passivation by carrier self-trapping," Phys. Rev. B. vol. 83, pp. 155207, April 2011.

[21] S. Chen, X. G. Gong, A. Walsh and S. H. Wei, "Crystal and electronic band structure of Cu_2ZnSnX_4 (X= S and Se) photovoltaic absorbers: first-principles insights," Appl. Phys. Lett. vol. 94, pp. 041903, January 2009.

[22] J. Vidal, S. Botti, P. Olsson, J. F. Guillemoles and L. Reining, "Strong interplay between structure and electronic properties in CuIn (S, Se)$_2$: a first-principles study," Phys. Rev. Lett. vol. 104, pp. 056401, February 2010.

[23] F. L. Tang, Z. X. Zhu, H. T. Xue, W. J. Lu, Y. D. Feng, Z. M. Wang and Y. Wang, "Optical properties of Al-doped CuInSe2 from the first principle calculation," Phys. Rev. B. Vol. 407, pp. 4814-4818, December 2012.

[24] A. Van de Walle, M. Asta and G. Ceder, "The alloy theoretic automated toolkit: A user guide," Calphad. vol. 26, pp. 539-553, December 2002.

[25] A. Van de Walle and M. Asta, "Self-driven lattice-model Monte Carlo simulations of alloy thermodynamic properties and phase diagrams," Modell. Simul. Mater. Sci. Eng. vol. 10, pp. 521, July 2002.

[26] A. Van de Walle and G. Ceder, "Automating first-principles phase diagram calculations," J PHASE EQUILIB vol. 23, pp. 348, September 2001.

[27] G. Kresse and J. Furthmüller, "Efficiency of ab-initio total energy calculations for metals and semiconductors using a plane-wave basis set," Comp. Mater. Sci. vol. 6, pp. 15-50, July 1996.

[28] G. Kresse and J. Furthmüller, "Efficient iterative schemes for ab initio total-energy calculations using a plane-wave basis set," Phys. Rev. B. vol. 54, pp. 11169-11186, October 1996.

[29] J. Yu, X. Lin, J. J. Wang, J. Chen and W. D. Huang, "First-principles study of the relaxation and energy of bcc-Fe, fcc-Fe and AISI-304 stainless steel surfaces," Appl. Surf. Sci. vol. 255, pp. 9032-9039, August 2009.

[30] L. C. Ma, J. M. Zhang and K. W. Xu, "Magnetic and electronic properties of Fe/Cu multilayered nanowires: a first-principles investigation," Physica. E. vol. 50, pp. 1-5, May 2013.

[31] G. Kresse and D. Joubert, "From ultrasoft pseudopotentials to the projector augmented-wave method," Phys. Rev. B. vol. 59, pp. 1758, January 1999.

[32] P. E. Blöchl, O. Jepsen and O. K. Andersen, "Improved tetrahedron method for Brillouin-zone integrations," Phys. Rev. B. vol. 49, pp.16233, June 1994.

[33] M. Gajdoš, K. Hummer, G. Kresse, J. Furthmüller and F. Bechstedt, "Linear optical properties in the projector-augmented wave methodology," Phys. Rev. B. vol. 73, pp. 045112, January 2006.

[34] D. Bhattacharyya, S. Chaudhuri and A. K. Pal, "Bandgap and optical transitions in thin films from reflectance measurements," Vacuum. vol. 43, pp.313-316, April 1992.

[35] H. T. Xue, F. L. Tang, F. Z Zhang, W. J. Lu and Y. D. Feng, "Temperature effects on distribution and inhomogeneous degree of In–Ga atoms in $CuIn_{1-x}Ga_xSe_2$ alloys," Mater. Lett. vol. 164, pp. 169-171, February 2016.

[36] H. T. Xue, F. L. Tang, F. Z Zhang, W. J. Lu and Y. D. Feng, "Effect of temperature on the distribution and inhomogeneity degree of Se-S atoms in $CuIn(Se_{1-x}S_x)_2$ alloys," J. Phys. D:Appl. Phys. vol. 49, pp. 025101, November 2015.